MICROWAVE ABSORPTION STUDY OF MULTIFUNCTIONAL GRAPHENE-BASED POLYLACTIDE

Dua, Mahima, and Mertiny, Pierre*
Department of Mechanical Engineering, University of Alberta, Edmonton, Canada
* Corresponding author (pmertiny@ualberta.ca)

Keywords*: graphene nanocomposites; thermoplastic polymer; microwave heating*

ABSTRACT

Thermoplastic polymer piping is widely used in the industry. Thermoplastics permit fusion bonding for the joining of pipe sections, which can be performed using joule heating. However, embedding heating wires into the plastic adds fabrication complexity and cost. Moreover, joule heating enables only localized heat input that requires moderation to avoid damage in low thermal conductivity polymers. Microwave heating may mitigate these shortcomings leading to shorter fusion times, enhanced heating uniformity, and lower electricity usage. This study explores the use of graphene nanoplatelets (GNP) to create multifunctional polylactide (PLA) composites for high microwave absorption. GNP/PLA composites were obtained via a two-step scalable fabrication procedure, consisting of solution blending followed by hot compression molding. The resulting composites were characterized for their thermal properties, electrical conductivity, and complex permittivity. Finally, microwave heating of GNP/PLA as a function of microwave power and filler loading was examined using thermal imaging. The produced nanocomposites were found to exhibit strong microwave absorption and thus rapid heating, making this type of composite a promising candidate for gasket materials that facilitate fusion bonding in thermoplastic-based piping.

1 INTRODUCTION

Despite global efforts to grow renewable energy generation, more than half of the total global energy need is supplied from the oil and gas industry [1]. As such, the safe and sustainable transportation of hydrocarbon products remains a critical issue. Metallic piping has a long history, with the oldest known use dating back to the third century in ancient Greece [2]. More recently, thermoplastic polymer piping is emerging as a viable alternative as it provides various advantages over metal pipes, including improved corrosion and fatigue resistance, chemical inertness, flexibility, a higher stiffness-to-weight ratio, and reduced installation and maintenance costs [2]–[4].

Thermoplastic polymer piping for high-pressure service is typically composed of an inner thermoplastic liner, a helically wrapped continuous reinforcement phase, and a thermoplastic outer jacket. The reinforcement phase, which can be dry fiber reinforcement or a polymer composite bonded or unbonded to the inner and outer thermoplastic layers, is the main load-bearing component of the thermoplastic polymer pipe. Common reinforcements are glass or carbon fibers, as well as metallic wires or bands [3].

Electrofusion welding via Joule heating is a method used for joining thermoplastic polymer pipes [5]. This process involves using couplings or fittings to surround the joint to be fused. Sending an electric current through metal coils inserted into the fittings produces heat and melts a portion of the pipes, resulting in the formation of a joint upon solidification. However, incorporating the metal coils into pipe components introduces complexity into the

manufacturing process. Failure mechanisms associated with electrofusion joints include misalignment of joints, incorrect dwell time for heating and cooling, and unsuitable welding, cooling and warming temperatures [6], [7]. In electrofusion welding of thermoplastic polymer pipes, it is recommended to work at temperatures above -15°C. Thus, in cold weather conditions this process must be carried out in shelters with temperatures maintained within an acceptable range, resulting in added cost and time-consuming processes [5]. Due to these limitations, innovative procedures are sought-after to effectively and expediently join piping made of advanced materials.

Microwave processing of materials is one such approach. Processing of materials via microwave energy has been proven to be a viable method for sintering [8], [9], joining [10], [11], cladding [12], [13], casting [14], [15], and drilling [16]–[18]. Microwave energy became a well-known method for material processing in the late 1990's [19]. Ever since, researchers have used this less-explored source of energy to process important engineering materials, including metals, ceramics, polymers, and their composites [20]. Microwave joining is a type of direct bonding technology that can offer various benefits over traditional joining methods, including quick processing, homogeneous temperature distribution, energy savings, environmental friendliness, welding of complicated geometries, high strength and enhanced joint microstructure [21]–[23].

Several studies on microwave processing have been reported in the technical literature. In a 2.45 GHz microwave unit, Wu and Benatar [24] used the microwave absorption capabilities of intrinsically conductive polyaniline polymer to weld microwave transparent high density polyethylene (HDPE) bars. Within 10 seconds a temperature of 300°C was attained, and a successful butt joint with a tensile strength comparable to bulk HDPE was attained in 60 seconds. To achieve microwave joining of thermoplastics, Wise and Froment [25] used a range of microwave-sensitive implants (including carbon-based implants as well as ceramic, polymer, and metal powder-based implants). They reported that carbon-based implants are most promising and cost-effective, taking only 3-60 seconds to create a joint. Wang et al. [26] joined polycarbonate substrates using multi-walled carbon nanotubes. A domestic microwave oven operating at 0.8 kW was used for this purpose and it took only 10 seconds to join the substrates. The bonding strength of the joint was found to be higher than that of the original polymer. In the work of Singh et al. [27], the joint strength of adhesively bonded joints and microwave-based joints was compared, and it was shown that the samples joined via microwave irradiation had higher joint strength than those made by adhesive bonding. Bajpai et al. [23] successfully performed microwave-assisted joining of a range of natural fibre reinforced polylactic acid (PLA, also known as polylactide) and polypropylene substrates using charcoal as the susceptor. Using a domestic microwave operating at 0.9 kW, lap joints were produced in 200-250 seconds.

The review of the technical literature revealed a gap relating to microwave absorption properties of multifunctional graphene-based PLA. PLA is an important thermoplastic polymer with high relevance in technical applications. More generally, this study explores the use of graphene nanoplatelets (GNP) to create multifunctional thermoplastic polymer composites for high microwave absorption. GNP/PLA composites were obtained via a two-step scalable fabrication procedure, consisting of solution blending followed by hot compression molding. The resulting composites were characterized for their thermal properties, electrical conductivity, and complex permittivity. Finally, microwave heating of GNP/PLA as a function of microwave power and filler weight fractions were examined using thermal imaging. Insights gained from the study of PLA based thermoplastics are intended to serve as a basis for the development of polymer composites for the microwave joining, specifically for thermoplastic piping products.

2 MICROWAVE HEATING MECHANISM

Microwave irradiation, i.e., high-frequency electromagnetic waves, can be used to heat a substance. While in traditional heating, heat is delivered externally to the material's surface, microwave irradiation penetrates and volumetrically heats the material [28]. This ensures that even thick materials are heated uniformly and quickly. The absorption of microwave energy is driven by the material permittivity and magnetic permeability, which account for time-harmonic electric and magnetic fields [19]. Not every material is appropriate for microwave heating, also known as dielectric heating, and the haphazard use of microwave irradiation in material processing may result in disappointment. The complex permittivity (ε*), see Equation (1), is the primary characteristic that describes the degree of heat generated in a non-magnetic material when interacting with microwave irradiation. The dielectric constant (ε') is the real part of the complex permittivity, and it represents a material's ability of being polarized by the microwave electric field, thus storing energy within the material. The dielectric loss factor (ε'') is the imaginary portion of the complex permittivity, and it represents the material's capacity to dissipate microwave energy into heat. The ability of a material to convert electromagnetic energy into heat is conveniently characterized by the dissipation factor or loss tangent, tan δ, see Equation (2) [29].

$$\varepsilon^* = \varepsilon' - j\varepsilon'' \quad (1)$$

$$\tan\delta = \varepsilon''/\varepsilon' \quad (2)$$

Considering microwave irradiation at a frequency of 2.45 GHz, common polymers have dielectric constants and dielectric loss factors ranging from 2.1 to 6.0 and from 0.0008 to 1.20, respectively [30]. On the other hand, polymer composites with a carbon black filler were shown to possess a dielectric constant and a dielectric loss factor of correspondingly 10.45 and 3.75, which indicates that carbon allotropes when used as filler can achieve much improved microwave absorption and heat conversion [31].

3 EXPERIMENTAL PROCEDURES

3.1 Materials

Graphene nanoplatelets (xGnP grade M15) were procured from XG Sciences (Lansing, MI, USA). Their average thickness, volumetric mass density, and electrical conductivity were, correspondingly, 6 to 8 nm, 2.2 g/cm^3, and 10^7 S/m parallel and 10^2 S/m perpendicular to the platelet plane. PLA was supplied in the form of pellets from Filabot Lab (type 4043D, Barre, VT, USA). The PLA glass transition temperature (T_g), volumetric mass density, and melting temperature range were specified by the supplier as 55 to 60°C, 1.24 g/cm^3, and 145 to 160°C, respectively. Fisher Scientific (Ottawa, ON, Canada) supplied with reagent grade chloroform and other chemicals.

3.2 Sample Preparation

3.2.1 GNP/PLA Nanocomposites

The GNP/PLA nanocomposites were prepared by solution mixing. Initially, PLA pellets and pristine GNP were dried in an oven at 80°C overnight. The next day, PLA and GNP were added to chloroform solvent forming two mixtures. The GNP mixture was treated with an ultrasonic processor for 3 hours (Q500, Qsonica, Newtown, CT, USA). The PLA mixture was mechanically stirred using an impeller agitator (Calframo, Georgian Bluffs, ON, Canada). After ultrasonication of the GNP mixture, both the mixtures were combined, sonicated for 60 minutes in an ice bath, and then transferred into a steel mold. The material was left in a fume hood for 12 hours to evaporate the solvent. The resultant films were dried in an oven at 120°C for 12 hours to eliminate any remnant solvent. Finally, the produced

material was compression molded into plates. Further details of the nanocomposite fabrication process can be found in [32]. Squares test samples were cut with dimensions of 25 mm and a thickness of 1.8 mm. For comparison, neat PLA samples were fabricated using comparable processes. Four types of materials with different GNP concentrations were prepared for testing as per Table 1.

Table 1. Composition of the nanocomposites.

GNP loading (wt%)	0	1	4	8
Material identifier	PLA	1-GNP/PLA	4-GNP/PLA	8-GNP/PLA

3.3 Material Characterization

3.3.1 Thermal Properties

The specific heat capacity (C_p) of the materials was measured by differential scanning calorimeter (model Q100, TA Instruments New Castle, DE, USA). Note that determining C_p is a necessary step for assessing the anisotropic thermal conductivity of the materials. Samples with a mass of 5 to 10 mg, prepared in platinum pans, were heated from 0°C to 200°C at a rate of 10°C/min under dry nitrogen flow (50 mL/min), in accordance with ASTM E1269-11 [33]. One test was conducted per filler weight fraction.

The anisotropic thermal conductivity of the materials was measured using a TPS2500S device (Thermtest, Fredericton, NB, Canada) with a Kapton sensor (type 5501, Thermtest). The sensor was sandwiched between two stacks of three samples of the same kind. Three test runs were conducted for each filler weight fraction, using a measurement duration and heating power set in accordance with IS0 22007-2 [34].

3.3.2 Electrical Conductivity

Material samples with a thickness and diameter of correspondingly 1 mm and 30 mm were prepared for electrical (volume) conductivity testing in dry air at room temperature. Samples with an electrical conductivity greater than 10^{-4} S/cm were examined by placing a four-pin probe at 90 V connected to a Loresta-GP resistivity meter (model MCP-T610, Mitsubishi Chemical, Osaka, Japan). For sample electrical conductivities less than 10^{-4} S/cm, a Hiresta-UP resistivity meter and UR type probe were used at 1000 V (Mitsubishi Chemical). One sample was tested for each filler loading.

3.3.3 Complex Permittivity

A vector network analyzer (ZVA67, Rohde & Schwarz, Munich, Germany) operating in a frequency range of 2.35 to 2.45 GHz connected to an open-ended coaxial probe was used to obtain the complex permittivity for each sample type. The stages of the open-ended coaxial technique calibration used were: ‘open circuit in air’, ‘short circuit with metal’, and ‘load in distilled water’. After complete calibration, polytetrafluoroethylene (PTFE) was used as the standard material to confirm the calibration prior to the start of a sample characterization. The sample to be measured was placed beneath the probe in such a manner that the probe tip was in direct contact with the sample without any air gap. Every sample was examined eight times, and the average value is reported.

3.4 Microwave Heating

A 2.45 GHz fixed frequency multimode applicator (NNST67KS, Panasonic, Osaka, Japan) with a maximum power output of 1.2 kW was used. The microwave chamber dimensions are 525 x 310 x 401 mm. A glass plate was placed inside the chamber on four ceramic supports at the corners. A specimen contained in a PTFE dish was placed at a distinct hotspot location on the glass plate inside the chamber. The hotspot location was determined using damp thermal paper. This arrangement is intended to create repeatable results in terms of sample placement and energy

input. Glass plates and PTFE dishes were exchanged between tests to ensure the same thermal conditions for each test. Power and time are the two key governing parameters in the microwave heating experiments. Specimens were irradiated at two different power levels, i.e., 0.6 kW and 1.2 kW. Microwave irradiation was halted after durations ranging from 3 to 180 seconds, or when melting of a specimen was observed. Following irradiation, the specimen with dish was removed rapidly from the chamber and placed on a wooden holder. An infrared camera (X8500sc, Teledyne FLIR, Wilsonville, OR, USA) was used to measure the specimen temperature distribution. For a given irradiation time and power level, single samples were tested for pure PLA and 1-GNP/PLA, while tests were conducted in triplicate for 4-GNP/PLA and 8-GNP/PLA, given that considerable data scatter was observed for the higher filler loadings.

4 RESULTS AND DISCUSSION

4.1 Thermal Properties

Referring to Table 2, the specific heat capacity was found to increase by 35.8% with the addition of 8 wt% GNP over the pure PLA matrix. In terms of thermal conductivity (see Figure 1A), neat PLA is isotropic with a value of 0.12 W/mK, which is consistent with values reported in the technical literature [35], [36].

Table 2. Specific heat capacity of PLA composites with different GNP filler weight fractions.

GNP loading (wt%)	0	1	4	8
Specific heat capacity (MJ/m^{3}K)	1.87	2.1	2.45	2.54

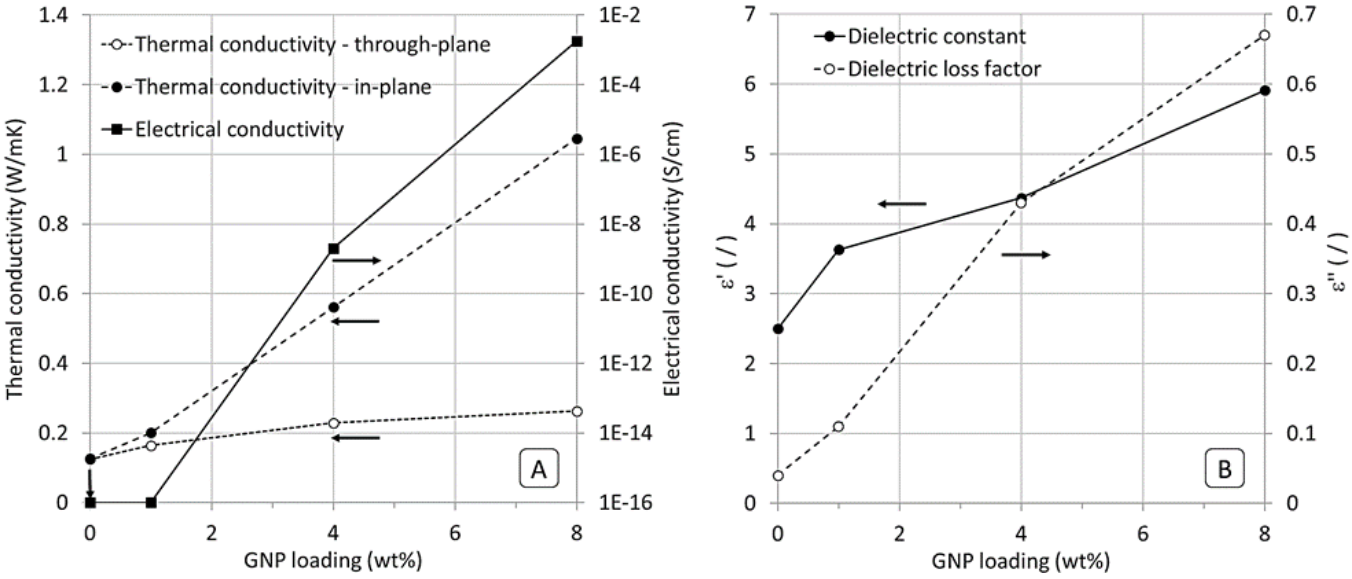

Figure 1. Thermal and electrical conductivity (A) and complex permittivity (B), i.e., dielectric constant ε' and dielectric loss factor ε'', for PLA composites with different GNP filler weight fractions.

As expected, increasing the GNP filler loading greatly improved thermal conductivity, particularly in the in-plane direction of the samples, yielding considerable anisotropy of the PLA/GNP nanocomposites. For instance, for 8-GNP/PLA samples the in-plane thermal conductivity reached a maximum value of 1.05 W/mK compared to 0.26 W/mK for the through-thickness direction. Notably, the in-plane thermal conductivity of 8-GNP/PLA nanocomposites increased by a factor of almost 7.5 over the pure PLA. The increase in thermal conductivity is attributed to the exceptionally high thermal conductivity of GNP compared to the polymeric matrix, as well as

possible network formation and interaction between graphene platelets as filler concentration increases, producing thermal conduction pathways. The latter can lead to reduced phonon scattering effects between polymer chains and filler particles [37]. The substantially higher in-plane thermal conductivity, compared to the through-thickness direction, can be explained by in-plane stacking effects of high-aspect ratio graphene platelets in the GNP/PLA nanocomposites. Similar trends were observed in [32], [38].

4.2 Electrical Conductivity

Electrical conductivity in polymers is caused by two factors: (i) Contact between particles in the composite forms paths for the conduction of electrical charge known as leakage current; and (ii) sufficiently close proximity of particles (in the nanometer scale) allows for the quantum mechanical phenomenon of electron tunneling to occur, thus permitting the conduction of electrical charge via a tunnelling current [39], [40].

As depicted in Figure 1A, electrical conductivity of PLA nanocomposites varied drastically as a function of GNP loading. While neat PLA and 1-GNP/PLA samples exhibited electrical conductivities below 10^{-16} S/cm, characterizing them as insulators, electrical conductivity jumped several orders of magnitude for the 4-GNP/PLA (~10^{-9} S/cm) and 8-GNP/PLA (~10^{-3} S/cm) nanocomposites. The latter can thus be characterized as a semiconductor rather than insulator material. Clearly, with rising GNP concentration, leakage and tunnelling currents increase owing to more physical contacts and shorter distances between platelets, respectively, with leakage current likely contributing to the conduction of charge to a greater extent than tunnelling current [41]. The significant rise in electrical conductivity with GNP loading is further attributed to percolation effects, i.e., the rapid formation of conductive pathways inside the material when exceeding certain filler loading threshold. In other research, percolating was found to occur when GNP concentration increased from 7 to 8 wt% [40] and 6 to 9 wt% [41].

4.3 Complex Permittivity

Polarization of charges inside a material influences its permittivity [42]. In polymers, permittivity is typically low; however, it can significantly be increased by the inclusion of conductive fillers [43]. Polarization of the matrix, conductive filler particles, and matrix/filler interface can all contribute to the overall permittivity of the composite in filled polymers [41], [42].

Figure 1B depicts the variation in the dielectric constant, ε', and dielectric loss factor, ε'', of the complex permittivity of PLA/GNP nanocomposites. The data show that permittivity of PLA nanocomposites is highly sensitive to GNP concentration. With rising GNP loading, ε' and ε'' exhibit similar rising trends, i.e., ε' and ε'' increased from 2.5 to 5.91 and 0.04 to 0.67 from neat PLA to 8-GNP/PLA samples, respectively.

The experimental findings agree with the technical literature. As discussed in [44], the inclusion of a conductive GNP filler increases the dipole moment and conductivity of PLA nanocomposites, resulting in considerable permittivity improvement. Other studies ([40], [41], [45]) reported similar increases in ε' and ε'' with increasing GNP loading. For example, ε' and ε'' were 8.5 and 0.9 for a 4 vol% GNP/epoxy nanocomposite at 1 GHz [45].

4.4 Microwave Heating

Figure 2A displays an example of a thermograph for a 1-GNP/PLA sample after heating at 1.2kW for 60 seconds. The thermograph demonstrate the expected volumetric heating of the nanocomposite materials, with temperatures reaching their maximum in the sample interior. Figure 2B depicts the (average) recorded temperatures for the various samples when irradiated for given times at 0.6 kW and 1.2 kW. In the case of pure PLA heated at 0.6 kW, the melting temperature (160°C) was not reached even after 180 seconds of irradiation. At 1.2 kW, however, the

sample reached the melting point within 180 seconds. The 1-GNP/PLA samples melted in within 180 seconds and 80 seconds at the low and high power levels, respectively. Notably, the 4-GNP/PLA and 8-GNP/PLA samples reached the melting point much more rapidly, within 15 seconds, for both power levels. For neat PLA and 1-GNP/PLA samples, an approximately linear temperature increase was observed until a rapid rise in temperature was noted approaching the melting point.

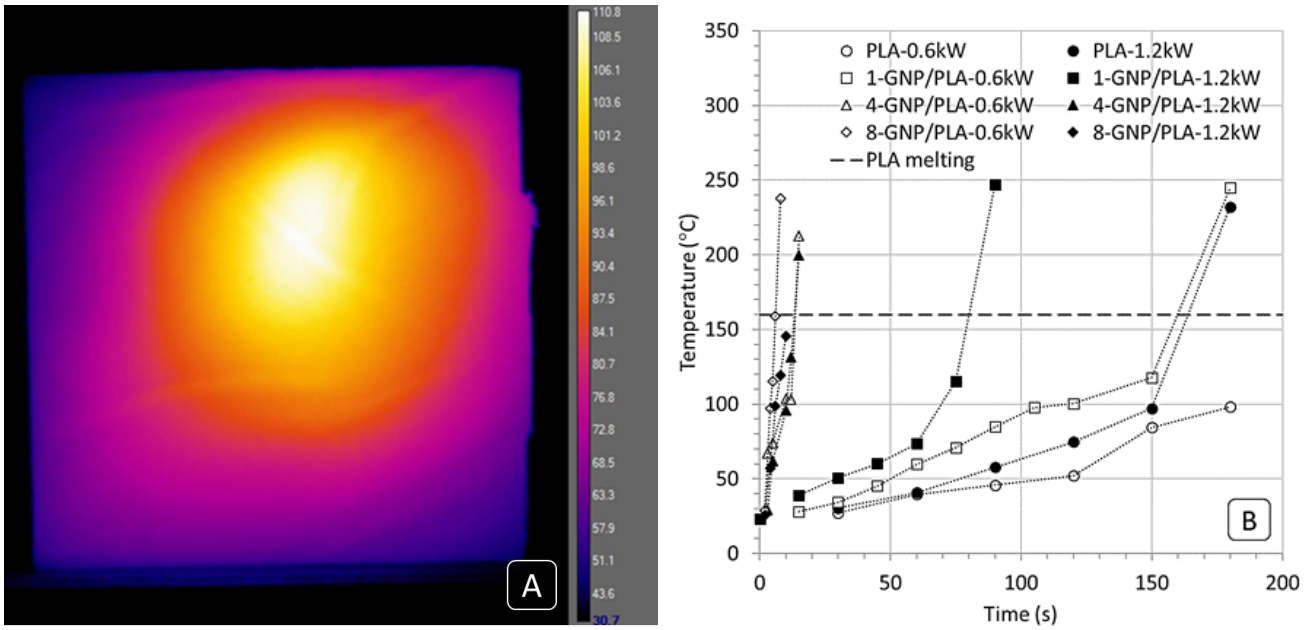

Figure 2. Example thermograph of a 1-GNP/PLA sample after heating at 1.2kW for 60 seconds (A), and measured average temperatures at different microwave irradiation durations for samples with different GNP filler weight fractions (B).

It is quite evident that upon adding GNP to the PLA matrix, the time taken to melt the material declines rapidly. Evidently, with increasing GNP loading, the nanocomposite shielding efficiency improves along with a rising electrical (and thermal) conductivity and permittivity [40][46]. An interesting finding is a diminishing return in GNP loading, i.e., beyond 4-GNP/PLA, heating a nanocomposite to the melting point occurs in mere seconds, which may even pose challenges in terms of process control to avoid overheating. In fact, considerable data scatter was observed for the 4-GNP/PLA and 8-GNP/PLA sample types, with standard deviations approaching 100°C in some instances (4-GNP/PLA and 0.6 kW). These effects may be related to the existence of filler agglomerates and percolated particle clusters exceeding 6 wt% GNP loading [32]. The observed rapid rise in temperature nearing the melting point may be due to the fact that the dielectric loss of composites increases with temperature, increasing heat generation [47]. A perplexing observation is that the 8-GNP/PLA samples, when heated at 0.6 kW, reached the melting point quicker than when heated at 1.2 kW. It is speculated when heating at 1.2 kW, rather than 0.6 kW, the 8-GNP/PLA material achieved the phase transition temperature rather rapidly, and the heat generated was unable to travel to lower temperature locations, reducing temperature uniformity and delaying the melting process. Lastly, the observed considerable data scatter is attributed largely to the type of microwave source used in these experiments, which was found to produce uneven irradiation power and heating, resulting in significant variation in results [48]. For future experimental studies, it is recommended to use a single-mode microwave source, which is more suited to maintain regulated power and homogeneous heating.

5 CONCLUSIONS

Multifunctional GNP/PLA nanocomposite samples with various GNP concentrations were fabricated in this work. Their thermal and electrical properties, complex permittivity, and microwave heating behavior as a function of microwave power and filler concentration, were studied. The results revealed that increasing GNP loading from nil to 8 wt% enhanced the specific heat capacity by 35.8%. The GNP/PLA nanocomposites exhibited anisotropic thermal behaviour, with the in-plane thermal conductivity of 8-GNP/PLA nanocomposites improving by a factor of almost 7.5 over pure PLA. In terms of electrical conductivity, pure PLA, with a value of less than 10^{-16} S/cm, was confirmed to be an insulator. In contrast, electrical conductivity for the 8-GNP/PLA nanocomposite increased several orders of magnitude (10^{-3} S/cm), making it a semiconductor material. The complex permittivity parameters, ε' and ε'', rose from 2.5 to 5.91 and 0.04 to 0.67 from the neat PLA to 8-GNP/PLA samples, respectively. When heated in a 2.45 GHz fixed frequency multimode applicator at 0.6 kW, the 8-GNP/PLA melted in mere 8 seconds, while pure PLA remained notably below the melting point even after 180 seconds or irradiation. The study revealed that increasing GNP filler loading to 4 wt% and 8 wt% substantially reduced the microwave heating time by over an order of magnitude compared to the pure polymer. However, a decreasing return in filler loading appears to exist beyond 4 wt%. The temperature rise was observed to be rapid, with poor reproducibility in test findings. Lastly, it was noted that when heating at 600W, 8-GNP/PLA reached the melting point somewhat faster than when heating at 1200W. In summary, the produced multifunctional GNP nanocomposites were shown to afford high microwave absorption and hence rapid heating, which indicates that thermoplastic GNP nanocomposites are a suitable choice for gasket materials that enable fusion bonding via microwave irradiation in thermoplastic-based components such as in piping systems.

6 ACKNOWLEDGEMENTS

The authors would like to express their appreciation to Drs. Ramin Khosravi and Rashid Mirzavand (University of Alberta) and Drs. Bahram Mirkhani and Uttandaraman Sundararaj (University of Calgary) for their assistance with assessing complex permittivity, and specific heat capacity and electrical conductivity, respectively.

7 REFERENCES

[1] *Key World Energy Statistics 2020 – analysis*. IEA. (n.d.). Retrieved April 04, 2022, from https://www.iea.org/reports/key-world-energy-statistics-2020.

[2] K. Yu, E. V Morozov, M. A. Ashraf, and K. Shankar. “A review of the design and analysis of reinforced thermoplastic pipes for offshore applications”. *Journal of Reinforced Plastics and Composites*, Vol. 36, No. 20, pp 1514-1530, 2017.

[3] A. Avery and S. Martin. “Reinforced Thermoplastic Pipe - Innovative technology for onshore field developments”. *Proceedings of International Conference on Offshore Mechanics and Arctic Engineering*, Vol. 36835, pp 787-794, 2003.

[4] T. Kadumberi, A. Prakash, R. O'Leary, and A. Gachagan. “Ultrasonic Imaging of Electrofusion Welded Polyethylene Pipes Employed in Utilities Industry”. *Proceedings of 51st Annual Conference of the British Institute of Non-Destructive Testing*, Northampton, pp 129-139, 2012.

[5] N. Starostin and R. Tikhonov. “Thermoelastic state during electrofusion welding of polyethylene pipes at different ambient temperatures”. Proceedings of IOP Conference Series: Earth and Environmental Science, Novosibirsk, Vol. 991, No. 1, 2022.

[6] D. S. Sarambale and D.K.Shinde. “Electro-fusion joint failure polyethylene pipes analysis and its simulation using finite element”. *International Journal of Mechanical and Production Engineering*, Vol. 5, No. 12, pp 51–55, 2017.

[7] A. Tutunchi, M. Eskandarzade, R. Aghamohammadi, T. Masalehdan, and K. Osouli-Bostanabad. “Risk assessment of electrofusion joints in commissioning of polyethylene natural gas networks”. *International Journal of Pressure Vessels and Piping*, Vol. 196, 2022.

[8] P. R. Matli, R. A. Shakoor, A. M. A. Mohamed, and M. Gupta. “Microwave rapid sintering of al-metal matrix composites: A review on the effect of reinforcements, microstructure and mechanical properties”. *Metals*, Vol. 6, No. 7, pp 1-19, 2016.

[9] J. Cheng, D. Agrawal, Y. Zhang, and R. Roy. “Microwave sintering of transparent alumina”. *Materials Letters*, Vol. 56, No. 4, pp 587–592, 2002.

[10] M. S. Srinath, A. K. Sharma, and P. Kumar. “A new approach to joining of bulk copper using microwave energy”. *Materials & Design*, Vol. 32, No. 5, pp 2685–2694, 2011.

[11] M. S. Srinath, A. K. Sharma, and P. Kumar. “Investigation on microstructural and mechanical properties of microwave processed dissimilar joints”. *Journal of Manufacturing Processes*, Vol. 13, No. 2, pp 141–146, 2011.

[12] S. Zafar and A. K. Sharma. “Development and characterisations of WC-12Co microwave clad”. *Material Charactization*, Vol. 96, pp 241–248, 2014.

[13] D. Gupta and A. K. Sharma. “Development and microstructural characterization of microwave cladding on austenitic stainless steel”. *Surface and Coatings Technology*, Vol. 205, No. 21–22, pp 5147–5155, 2011.

[14] R. R. Mishra and A. K. Sharma. “On mechanism of in-situ microwave casting of aluminium alloy 7039 and cast microstructure”. *Materials & Design*, Vol. 112, pp 97–106, 2016.

[15] R. R. Mishra and A. K. Sharma. “A Review of Research Trends in Microwave Processing of Metal-Based Materials and Opportunities in Microwave Metal Casting”. *Critical Reviews in Solid State and Materials Sciences*, Vol. 41, No. 3, pp. 217–255, 2016.

[16] A. Singh and A. K. Sharma. “On microwave drilling of metal-based materials at 2.45 GHz”. *Applied Physics A: Materials Science & Processing*, Vol. 126, No. 10, pp 1–11, 2020.

[17] N. K. Lautre, A. K. Sharma, P. Kumar, and S. Das. “Microwave Drilling with Litz Wire using a Domestic Applicator”. *Bonfring International Journal of Industrial Engineering and Management Science*, Vol. 4, No. 3, pp 125–131, 2014.

[18] T. J. George, A. K. Sharma, and P. Kumar. “Experimental Study and Simulation on Microwave Drilling of Metals and Glasses”. *Journal of Experimental & Applied Mechanics*, Vol. 5, No. 1, pp 10–19, 2014.

[19] R. R. Mishra and A. K. Sharma. “Microwave-material interaction phenomena: Heating mechanisms, challenges and opportunities in material processing”. *Composites Part A: Applied Science and Manufacturing,* Vol. 81, pp. 78–97, 2016.

[20] D. E. Clark, D. C. Folz, and J. K. West. “Processing materials with microwave energy”. *Materials Science and Engineering: A*, Vol. 287, No. 2, pp 153–158, 2000.

[21] T. P. Naik, I. Singh, and A. K. Sharma. “Processing of polymer matrix composites using microwave energy: A review”. *Composites Part A: Applied Science and Manufacturing*, Vol. 156, 2022.

[22] M. K. Singh and S. Zafar. “Influence of microwave power on mechanical properties of microwave-cured polyethylene/coir composites”. *Journal of Natural Fibers*, Vol. 17, No. 6, pp 845–860, 2020.

[23] P. K. Bajpai, I. Singh, and J. Madaan. “Joining of natural fiber reinforced composites using microwave energy: Experimental and finite element study”. *Materials & Design,* Vol. 35, pp 596–602, 2012.

[24] C. Wu and A. Benatar. “Microwave welding of high density polyethylene using intrinsically conductive polyaniline”. *Polymer Engineering & Science*, Vol. 37, No. 4, pp 738–743, 1997.

[25] R. J. Wise and I. D. Froment. “Microwave welding of thermoplastics”. *Journal of materials science*, Vol. 36, No. 24, pp 5935–5954, 2001.

[26] C. Wang, T. Chen, S. Chang, S. Cheng, and T. Chin. “Strong carbon-nanotube-polymer bonding by microwave irradiation”. *Advanced Functional Materials*, Vol. 17, No. 12, pp 1979–1983, 2007.

[27] I. Singh, P. K. Bajpai, D. Malik, J. Madaan, and N. Bhatnagar. “Microwave joining of natural fiber reinforced green composites”. *Advanced Materials Research,* Vol. 410, pp 102–105, 2012.

[28] W. Cha-um, P. Rattanadecho, and W. Pakdee. “Experimental analysis of microwave heating of dielectric materials using a rectangular wave guide (MODE: TE10) (Case study: Water layer and saturated porous medium)”. *Experimental Thermal and Fluid Science*, Vol. 33, No. 3, pp 472–481, 2009.

[29] H. S. Ku, F. Siu, E. Siores, J. A. R. Ball, and A. S. Blicblau. “Applications of fixed and variable frequency microwave (VFM) facilities in polymeric materials processing and joining,” *Journal of Materials Processing Technology*, Vol. 113, No. 1-3, pp 184–188, 2001.

[30] M. Gupta and W. W. L. Eugene. "*Microwaves and Metals*". John Wiley & Sons, 2008.

[31] G. Arora, H. Pathak, and S. Zafar. “Fabrication and characterization of microwave cured high-density

polyethylene/carbon nanotube and polypropylene/carbon nanotube composites". *Journal of Composite Materials*, Vol. 53, No. 15, pp 2091–2104, 2019.

[32] Q. Zhang and P. Mertiny. "Effect of Graphene Nanoplatelet Addition on the Conductive Behavior of Solution Mixing Processed Polylactide Biopolymer Nanocomposites". *Proceedings of the ASME 2019 International Mechanical Engineering Congress and Exposition, Salt Lake City, Utah, USA, Volume 12: Advanced Materials: Design, Processing, Characterization, and Applications*, 2019.

[33] ASTM E1269-11. "Standard test method for determining specific heat capacity by differential scanning calorimetry". *ASTM International* (2011). Reapproved, 2018.

[34] ISO 22007-2: 2015. " Plastics – determination of thermal conductivity and thermal diffusivity – Part 2: transient plane heat source (hot disc) method". International Organization for Standardization (ISO), Switzerland (2015)

[35] A. Haleem, V. Kumar, and L. Kumar. "Mathematical Modelling & Pressure Drop Analysis of Fused Deposition Modelling Feed Wire". *International Journal of Engineering Technology*, Vol. 9, No. 4, pp 2885–2894, 2017.

[36] O. Zmeskal, L. Marackova, T. Lapcikova, P. Mencik, and R. Prikryl. "Thermal properties of samples prepared from polylactic acid by 3D printing". *AIP Conference Proceedings*, Vol. 2305, 2020.

[37] K. Ruan, Y. Guo, and J. Gu. "Liquid Crystalline Polyimide Films with High Intrinsic Thermal Conductivities and Robust Toughness". *Macromolecules*, Vol. 54, No. 10, pp 4934–4944, 2021.

[38] Y. Pan *et al.* "Enhanced Thermally Conductive and Microwave Absorbing Properties of Polymethyl Methacrylate/Ni@GNP Nanocomposites". *Industrial & Engineering Chemistry Research*, Vol. 60, No. 33, pp 12316–12327, 2021.

[39] J. Chang, G. Liang, A. Gu, S. Cai, and L. Yuan. "The production of carbon nanotube/epoxy composites with a very high dielectric constant and low dielectric loss by microwave curing". *Carbon*, Vol. 50, No. 2, pp 689–698, 2011.

[40] S. Kashi, R. K. Gupta, T. Baum, N. Kao, and S. N. Bhattacharya. "Morphology, electromagnetic properties and electromagnetic interference shielding performance of poly lactide/graphene nanoplatelet nanocomposites". *Materials & Design*, Vol. 95, pp 119–126, 2016.

[41] S. Kashi, R. K. Gupta, T. Baum, N. Kao, and S. N. Bhattacharya. "Dielectric properties and electromagnetic interference shielding effectiveness of graphene-based biodegradable nanocomposites". *Materials & Design*, Vol. 109, pp 68–78, 2016.

[42] A. Ameli, P. U. Jung, and C. B. Park. "Electrical properties and electromagnetic interference shielding effectiveness of polypropylene / carbon fiber composite foams". *Carbon*, Vol. 60, pp 379–391, 2013.

[43] S. Wai, M. Tadokoro, J. Watanabe, and N. Kuramoto. "Microwave absorption behaviors of polyaniline nanocomposites containing TiO 2 nanoparticles". *Current Applied Physics*, Vol. 8, No. 3-4, pp 391–394, 2008.

[44] A. Gupta and V. Choudhary. "Electromagnetic interference shielding behavior of poly (trimethylene terephthalate)/ multi-walled carbon nanotube composites." *Composites Science and Technology*, Vol. 71, No. 13, pp 1563–1568, 2011.

[45] S. E. Lee, O. Choi, and H. T. Hahn. "Microwave properties of graphite nanoplatelet/epoxy composites". *Journal of Applied Physics*, Vol. 104, No. 3, 20108.

[46] M. Omran, T. Fabritius, G. Chen, and A. He. "Microwave absorption properties of steelmaking dusts: Effects of temperature on the dielectric constant (ε') and loss factor (ε'') at 1064 MHz and 2423 MHz". *RSC advances*, Vol. 9, No. 12, pp 6859–6870, 2019.

[47] K. Liu, X. Xu, and B. Zhang. "Characterization and simulation of the nonlinear thermal field of the aramid/bismaleimide composites caused by the dielectric heating effects of the microwave radiations". *Polymer Composites*, Vol. 42, No. 5, pp 2565–2573, 2021.

[48] Z. Han, Y. Li, D. H. Luo, Q. Zhao, J. H. Cheng, and J. H. Wang. "Structural variations of rice starch affected by constant power microwave treatment," *Food Chemistry*, Vol. 359, 2021.